J Mater Sci: Mater Med (2010) 21:797–805
DOI 10.1007/s10856-009-3873-3

Selected physicochemical properties of the experimental endodontic sealer

J. I. Johns · J. N. R. O'Donnell · D. Skrtic

Received: 2 July 2009 / Accepted: 9 September 2009 / Published online: 19 September 2009

Abstract This study explores water sorption, hygroscopic expansion, mechanical strength and ion release from the experimental amorphous calcium phosphate (ACP) composites formulated for application as endodontic sealers. Light-cure (LC) and dual-cure (DC; combined light and chemical cure) resins comprised urethane dimethacrylate (UDMA), 2-hydroxyethyl methacrylate (HEMA), methacryloyloxyethyl phthalate (MEP) and a high molecular mass oligomeric co-monomer, poly(ethyleneglycol)-extended UDMA (PEG-U) (designated UPHM resin). To fabricate composites, a mass fraction of 60% UPHM resin was blended with a mass fraction of 40% as-made (am-) or ground (g-) ACP. Glass-filled composites were used as controls. Both DC and LC ACP UPHM composites exhibited relatively high levels of water sorption accompanied by a significant hygroscopic expansion. The latter may potentially be useful to offset high polymerization stresses that develop in these materials. Ion release profiles of the experimental materials confirmed their potential for regeneration of mineral-deficient tooth structures. Their moderate to low mechanical strength after 3 months of aqueous immersion did not diminish the enthusiasm for the proposed use as endodontic sealers. For that application, DC g-ACP composites appear to be the most adequate, but micro-leakage and quantitative leachability studies are needed to fully establish their suitability.

Disclaimer: Certain commercial materials and equipment are identified in this work for adequate definition of the experimental procedures. In no instance does such identification imply recommendation or endorsement by the American Dental Association Foundation or the National Institute of Standards and Technology, or that the material and the equipment identified is necessarily the best available for the purpose.

J. I. Johns · J. N. R. O'Donnell · D. Skrtic (✉)
Paffenbarger Research Center, American Dental Association Foundation, National Institute of Standards and Technology, 100 Bureau Drive Stop 8546, Gaithersburg, MD 20899-8546, USA
e-mail: drago.skrtic@nist.gov

1 Introduction

Calcium phosphates (CaPs) are of significant interest to the dental field due to their involvement in both normal dentition as well as in pathological mineralization (dental calculus) and demineralization (dental caries) [1]. Amorphous calcium phosphate (ACP), a unique, non-crystalline CaP that forms spontaneously from supersaturated basic Ca and PO_4 solutions, is generally viewed as both an in vitro and in vivo precursor to thermodynamically stable hydroxyapatite (HAP) [2, 3]. The rate of ACP conversion to HAP, dictated by the chemistry of the microenvironment, is affected by the presence of inorganic anions, cations, or organic molecules which can adsorb on the ACP surface, incorporate into the ACP structure and/or co-precipitate with ACP. This conversion is accompanied by the concomitant release of Ca and PO_4 ions needed to reform damaged mineral structures, thus giving ACP-based materials the potential to counteract the recurrent decay known to develop near the surfaces of teeth in contact with conventional fillings (almost 50% of all dental fillings require replacement because of recurrent caries). When embedded in polymerized methacrylate matrices [4, 5] and exposed to an aqueous environment, ACP releases sufficient levels of remineralizing ions in a sustained manner to effectively regenerate mineral-deficient enamel lesions [6, 7]. A problem with dental composites of all types is the development of internal and interfacial stresses due to volumetric contraction upon polymerization. Additionally,

ACP composites have low fracture resistance under masticatory stress due to their low strength and toughness. The uncontrolled aggregation of ACP particles was identified as the main cause of the poor interfacial ACP/resin interactions leading to the inferior mechanical performance of ACP composites in comparison to glass-reinforced composites [8, 9]. As a result of our efforts to improve the ACP filler/polymer matrix interfacial properties by better controlling the particle size distribution and surface properties of ACP fillers and by fine-tuning the resin [4, 8, 10, 11], an ACP pit and fissure sealant and orthodontic adhesive have been successfully formulated. Most recently we have focused our research on designing a remineralizing ACP endodontic sealer. Successful completion of this project would widen ACP's clinical significance beyond topical gels, toothpastes and/or mouthrinses [12], sugar-free chewing gums and glass ionomers [13, 14], as well as the more recently developed ACP composites based on our ACP-composite technology [15].

Recently formulated light-cure (LC) and dual cure (DC; light plus chemical) urethane dimethacrylate-based, remineralizing ACP polymeric composites attained high degrees of double bond conversion (DVC) accompanied with relatively high polymerization shrinkage and moderate levels of polymerization stress [16]. High DVCs attained in these materials suggest low leachability of the un-reacted monomeric species, and imply low probability of adverse cellular responses. However, the extensive shrinkage/stress seen in these composites might present a serious clinical risk because it increases probability of developing strains and gaps in the microstructure of composite and at the composite/dentin interface that could act as potential sites for microleakage. In clinical settings, dental materials are continuously exposed to water from the oral environment. The water uptake that softens and degrades the resin matrix [17, 18] may also allow for the relaxation of residual stresses that develop within the matrix during the polymerization shrinkage [19–21], and decrease or close marginal leakage gaps [22, 23]. We hypothesize that LC and/or DC composites made from Zr-ACP filler and urethane dimethacrylate (UDMA)/poly(ethyleneglycol)-extended UDMA (PEG-U)/2-hydroxyethyl methacrylate (HEMA)/methacryloyloxyethyl phthalate (MEP) resin (designated UPHM resin) will exhibit relatively high (WS) accompanied with significant hygroscopic expansion of composite specimens. The latter may offset the high volumetric shrinkage seen in these composites [16]. It is expected that the relatively high WS will not diminish composites' mechanical strength more than is customarily seen in other types of ACP methacrylate composites, and that ion release from composites will result in solution supersaturations required for efficient mineral recovery [4, 6, 7]. To test these hypotheses, we extend the physicochemical evaluation of the experimental endodontic ACP composites [16] to WS, hygroscopic expansion, mechanical strength and ion release measurements during the mid-term exposure of copolymer and composite specimens to aqueous environment.

2 Materials and methods

2.1 Synthesis and characterization of ACP filler

Zirconia-hybridized ACP (assigned am-ACP) was synthesized as described in detail in Refs. [4, 8, 15]. Grinding of am-ACP was performed according to the procedure detailed in Ref. [16]. Both am- and ground (g-ACP) filler were routinely characterized by X-ray diffraction (XRD), Fourier-transform Infrared (FTIR) spectroscopy, particle size distribution (PSD) analysis and scanning electron microscopy (SEM). Methodological details on XRD, FTIR, PSD and SEM analysis are provided in Refs. [4, 5, 7–11].

2.2 Resin formulation

Resins were formulated from commercial UDMA, PEG-U, HEMA and MEP monomers, with photo- and/or chemical-initiators added according to the system: light-cure (LC UPHM resin) or dual cure (DC UPHM resin). Compositions of the LC and DC resins, as well as the acronyms used throughout this manuscript are provided in Table 1. After introducing the appropriate initiators to the monomer blends, the activated resin mixtures were magnetically stirred until fully homogenized.

2.3 Preparation of copolymer and composite specimens

LC copolymer (the unfilled resin) specimens (disks with an average diameter (12.91 ± 0.13) mm and thickness (1.44 ± 0.16) mm) were prepared by irradiating photo-activated resins for 60 s (Triad 2000; Dentsply International, York, PA, USA). In DC series, 1850 IRGACURE- and BPO-containing resin was combined with DHEPT-containing resin (1:1 mass ratio) to initiate chemical polymerization and then additionally light-cured under conditions identical to LC systems. Composite pastes were prepared by hand-mixing UPHM resin (mass fraction 60%) and either am- or g-ACP (mass fraction 40%) until a uniform consistency was achieved. The homogenized pastes were spread thinly on a dental slab (flat glass block) and kept under moderate vacuum (2.7 kPa) to eliminate the air entrained during mixing. Composite specimens were cured in the same manner as copolymer samples. Control composite specimens were made with unsilanized Sr-glass (Dentsply Caulk, Milford, DE, USA). To achieve a consistency comparable to

Table 1 The composition of light-cure (LC) and dual cure (DC) UPHM resin used in the study

Monomer or component of the polymerization initiator system	Acronym	Mass%	
		LC	DC[a]
Urethane dimethacrylate	UDMA	48.7	47.2
Poly(ethyleneglycol)-extended UDMA	PEG-U	30.0	29.1
2-hydroxyethyl methacrylate	HEMA	17.3	16.8
Methacryloyloxyethyl phthalate	MEP	3.0	2.9
Camphorquinone	CQ	0.2	–
Ethyl-4-*N,N*-dimethylamino benzoate	4EDMAB	0.8	–
Bis(2,6-dimethoxynezoyl)-2,4,4-triethylpentyl	1850 IRGACURE	–	1.0
Phosphine oxide & 1-hydroxycyclohexyl phenyl ketone benzoyl peroxide	BPO	–	2.0
2,2′-dihydroxyethyl-*p*-toluidine	DHEPT	–	1.0

[a] DC resin was fabricated by mixing equal amounts by mass of the UPHM resin containing 1850 IRGACURE and BPO with the UPHM resin containing DHEPT

ACP-composites, 70 mass% glass was blended with the resin in these control specimens.

2.4 Water sorption (WS) and dimensional changes upon aqueous immersion

To determine WS profiles of copolymers and composites, a minimum of nine specimens per each experimental group were initially dried over anhydrous $CaSO_4$ until a constant mass was achieved (±0.1 mg). Specimens were then exposed to an air atmosphere of 75% relative humidity (RH) at 23°C by keeping them suspended over saturated aqueous sodium chloride slurry in closed systems. Mass changes of dry-padded specimens were recorded at predetermined time intervals. The relative degree of WS of each individual specimen at any given time interval (t), expressed as a mass% fraction, was calculated using a simple equation:

$$\mathrm{WS} = [(W_t - W_o)/W_o] \times 100 \quad (1)$$

where W_t represents a specimen mass at time t and W_o is the initial mass of dry specimen.

In addition to WS measurements at 75% RH, a minimum of five disk specimens in each experimental group were immersed in 25 ml of 4-(2-hydroxyethyl)-1-piperazineethanesulfonic acid (HEPES)-buffered, pH = 7.4, 0.13 mol/l sodium chloride (saline) solution at 23°C and their mass (determined gravimetrically), diameter and thickness (measured by micrometer) were recorded at different times of immersion. Mass and dimensional data were used to calculate relative mass (Δ mass%) and volume (Δ vol.% = hygroscopic expansion) changes (applying the same relationship as defined in Eq. 1 to the mass and volume (cylindrical disk geometry) of the samples at time t vs. the initial mass and volume, respectively.

2.5 Mechanical testing of the copolymers and composites

To compare the mechanical strength of dry (kept in the air 24 h at 23°C) and wet (after 3 months immersion in saline solution at 23°C) copolymer and composite specimens, their biaxial flexure strength (BFS) was determined using a computer-controlled Universal Testing Machine (Instron 5500R, Instron Corp., Canton, MA, USA) operated by Instron Merlin Software series 9. BFS of disk specimens (n = 5/group) supported along a lower support circle was determined under a static load utilizing a piston-on-three-ball loading arrangement with a cross head speed of 0.5 mm/min. The failure stress was calculated according to the ASTM specification F394-78 [24].

2.6 Calcium and phosphate release from composites

Mineral ion release from ACP composite disk specimens was assessed at 23°C, in magnetically stirred, HEPES-buffered saline solutions (25 ml saline/specimen). Saline solution was replaced at predetermined time intervals (up to 3 months). The kinetic changes in calcium and phosphate concentrations were determined by utilizing atomic emission spectroscopy (Prodigy High Dispersion ICP-OES, Teledyne Leeman Labs, Hudson, NH, USA).

Calcium and phosphate solution concentration data were recalculated as the rate of release ($\Delta Ca/\Delta t$ or $\Delta PO_4/\Delta t$ (in mmol/day)), and plotted against time according to a power law equation of general type:

$$\Delta c/\Delta t = a \times t^k \quad (2)$$

or, in its logarithmic form

$$\log\left(\frac{\Delta c}{\Delta t}\right) = \log a + k \log t \quad (3)$$

where Δc represents a change in calcium or phosphate concentration, Δt is a time interval, a is a constant of proportionality, k is the scaling exponent, and t is the immersion time.

2.7 Statistical analysis

The results were analyzed by the analysis of variance (ANOVA; $\alpha = 0.05$). Statistical significance of change values was obtained from two-tailed P values using the Holm–Sidak test for paired data. Statistical calculations were done by means of SigmaStat software (version 3.5; SPSS Inc., Chicago, IL, USA). One standard deviation (SD) is identified in this paper for comparative purposes as the estimated uncertainty of the measurements.

3 Results

3.1 Physicochemical characteristics of ACP fillers

Results of the physicochemical characterization of am-ACP and g-ACP filler are summarized in Table 2. While exhibiting the identical XRD patterns and FTIR spectra, am-ACP and g-ACP filler differed significantly with respect to their PSD. As a result of being significantly less agglomerated than am-ACP, g-ACP easily blended at a 40% mass fraction with UPHM resin and yielded highly flowable paste. On the other hand, am-ACP required prolonged hand spatulation and produced a viscous, essentially non-flowable paste. The unsilanized Sr glass used in control LC composites had a relatively uniform PSD (particles ranging from 0.1 to 5 μm) and $d_m = (1.3 \pm 0.09)$ μm. A minimum of almost 70 mass% Sr-glass was required in the composite mixture to achieve consistency comparable to that of g-ACP composites while still being more flowable than am-ACP counterparts.

3.2 Mechanical strength of copolymers and composites

The mechanical strength of dry and wet copolymers and composites is compared in Fig. 1. In both dry state and after aqueous immersion, the unfilled LC and DC UPHM copolymers exhibited significantly higher biaxial flexural strength (BFS) than the BFS of LC control glass composite and the BFS of LC and DC ACP composites fabricated with either am- or g-ACP. The copolymers also exhibited the highest extent of BFS reduction in going from dry to wet specimens (≤43%) compared to the BFS reduction in am-ACP composites (≤28%), g-ACP composites (≤21%) and glass control (≤13%). The differences between the

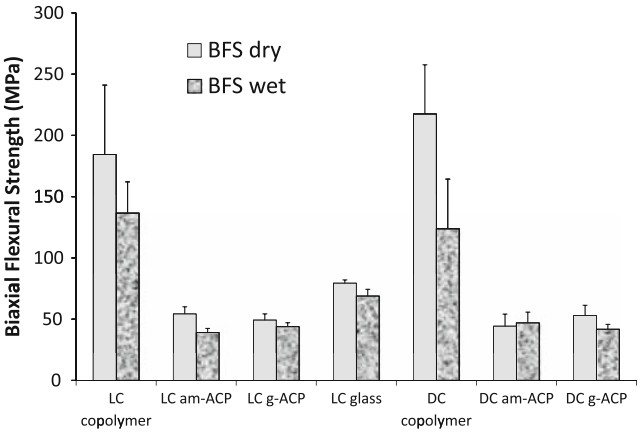

Fig. 1 Biaxial flexural strength (BFS; mean value ± standard deviation (SD)) of dry and wet UPHM copolymers and their light cure (LC) and dual cure (DC) am-ACP and g-ACP composites. Glass-filled composite is taken as a control in LC series. The number of specimens in each experimental group $n \geq 5$

Table 2 Physicochemical characteristics of the ACP fillers utilized in the study

Method	Physical property	Instrument/manufacturer	Findings
X-ray diffraction (XRD)	Long-range structural order	DMAX2000; Rigaku/USA Inc., MA, USA	*am- and g-ACP*: two diffuse broad bands in $2\theta(^\circ) = 4$–60 region
Fourier-transform infrared spectroscopy (FTIR)	Short-range structural environment	Nicolet Magna FTIR System 550; Nicolet Instrument Corp., WI, USA	*am- and g-ACP*: phosphate stretching absorption band at (1200–900) cm^{-1} and phosphate bending band at (630–500) cm^{-1}
Particle size distribution (PSD)	Volume and number PSD; median (d_m) particle size	CIS-100 Particle Size Analyzer; Ankersmid Ltd., Yokneam, Israel	*am-ACP*: particle sizes up to 270 μm; $d_m = (75 \pm 5)$ μm *g-ACP*: particle sizes up to 11 μm; $d_m = (5 \pm 1)$ μm
Scanning electron microscopy (SEM)	Morphology, topology, size	JSM-5400; JEOL, Inc., MA, USA	*am-ACP*: large agglomerates (≤ 200 μm) and some finer particles; *g-ACP*: smaller agglomerates (≤ 20 μm) and prevalently fine particles

BFS of both dry and wet LC and DC am- and g-ACP composites were not statistically significant.

3.3 Mass changes of copolymers and composites at 75% relative humidity

Mass changes of copolymer and composite specimens caused by water sorption at 75% relative humidity (RH) are shown in Fig. 2. Rapid water uptake occurred within the initial 336 h of exposure to 75% RH. Plateau, WS_{max} values were reached in all systems at time intervals ≥336 h are compared in Fig. 3. They decreased in the following order: [LC (am-ACP, g-ACP, copolymer)] > [DC (am-ACP, g-ACP, copolymer] > LC glass.

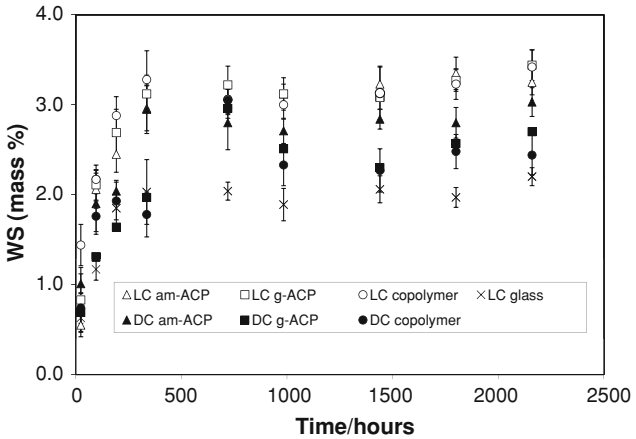

Fig. 2 Kinetic changes in water sorption (WS) values (mean ± SD) of copolymer and composite specimens exposed to 75% relative humidity (RH) at room temperature for up to 90 days. The number of specimens in each experimental group $n \geq 9$

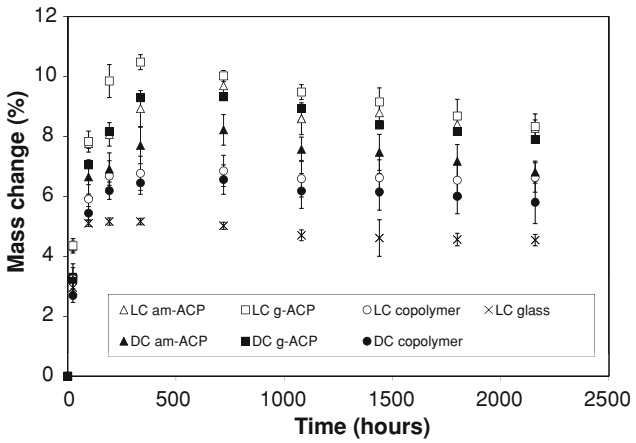

Fig. 3 Increases in specimen mass, expressed as mass % of the initial specimen mass, as a function of time for the copolymer and composite specimens immersed in buffered saline at room temperature for up to 90 days. Indicated are mean values ± SD for 5 samples/experimental group

3.4 Mass and volume changes of copolymers and composites upon aqueous immersion

Specimen mass increases occurring upon immersion in saline (Fig. 3) were on average 2.5–3.0 times higher compared to specimens exposed to relative humidity. Based on the multiple statistical comparisons (two-tail *t*-test; unequal variances), mass changes decreased in the following order: [LC (am-ACP, g-ACP); DC (g-ACP)] > DC (am-ACP) > LC (copolymer) > DC (copolymer) > LC glass. Contrary to the mass changes due to water sorption alone, masses of immersed specimens, after reaching the maximum between 336 and 720 h, showed a mild, but consistent, decreasing trend. The corresponding changes in specimens' volume calculated on the basis of the measured dimensional changes (cylindrical geometry) are shown in Fig. 4. Similar to the maximum mass changes, the maximum volume changes or hygroscopic expansion of the specimens decreased in the following order: [LC, DC (am-ACP, g-ACP)] > [LC, DC (copolymer)] > LC glass.

3.5 Ion release from composites

Kinetics profiles of calcium and phosphate released from am- and g-ACP UPHM composites (both LC and DC) are shown in Fig. 5a and 5b, respectively. As can be seen from this kinetic data, within 3 months of aqueous immersion, no plateau (maximum) concentration of either ion has yet been reached. The typical example of the ion release data recalculated as the change in calcium (or phosphate) solution concentration with time is shown in Fig. 6 (logarithmic form of a power law equation [4]). The *a* and *k* values calculated from the plots of all experimental data are listed in Table 3. Higher *a* values obtained for am-ACP formulations compared to g-ACP counterparts correlate

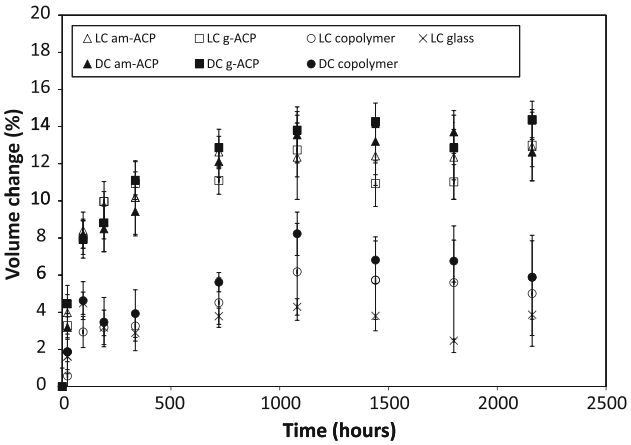

Fig. 4 Volume changes accompanying the mass increases shown in Fig. 3

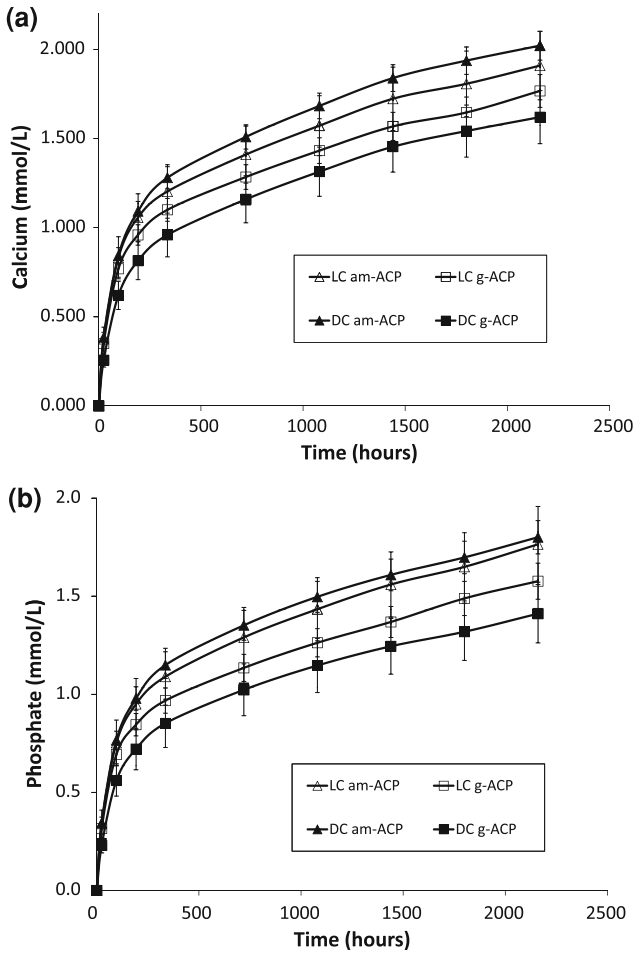

Fig. 5 Kinetic profiles of calcium (**a**) and phosphate (**b**) ion release from LC and DC UPHM composites formulated with am- and g-ACP. Indicated are mean values ± SD for three repetitive runs in each experimental group

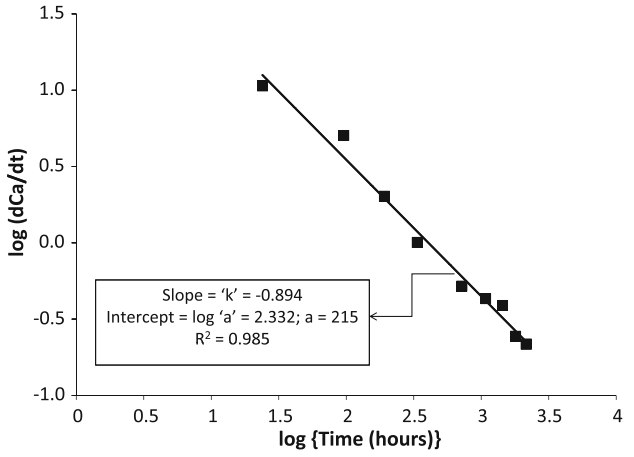

Fig. 6 General power law expression in its logarithmic form for the Ca release kinetic curve obtained with DC g-ACP composites

well with the moderately enhanced ion release rates seen in these composites. The levels of calcium and phosphate ions released into immersion solutions at 1 month, recalculated as the corresponding ion activity products (IAP) and the thermodynamic stability of these solutions are shown in Table 4. Independent of the type of cure or type of ACP filler, supersaturations attained in all of the solutions were significantly above the minimum necessary for mineral redeposition (saturation ratio SR > 1.00).

Table 3 Average values of a (a constant of proportionality) and k (the scaling exponent) calculated from the plots of log [Δ(Ca or PO_4)/Δt] against log t (general power law expression in its logarithmic form; example in Fig. 6) for all of the experimental data

	[Δ(Ca)/Δt] vs. time			[Δ(PO_4)/Δt] vs. time		
	a	k	R^2	a	k	R^2
LC am-ACP	349	−0.952	0.9789	278	−0.925	0.9779
g-ACP	288	−0.931	0.9700	234	−0.915	0.9710
DC am-ACP	392	−0.962	0.9901	331	−0.952	0.9867
g-ACP	215	−0.894	0.9849	189	−0.895	0.9810

R correlation coefficient

Table 4 Comparison of the ion activity product (IAP) and the saturation ratio (SR) with respect to stoichiometric hydroxyapatite ($Ca_{10}(OH)_2(PO_4)_6$; HAP) and enamel attained in the immersing solutions as a result of calcium and phosphate ion release from composite specimens being immersed for 1 month

Resin	Filler	$pK_{IAP} = -\log(IAP)$	SR_{HAP}	SR_{enamel}
LC UPHM	am-ACP	97.1	12.5	4.4
	g-ACP	97.7	11.5	4.0
DC UPHM	am-ACP	96.7	13.2	4.6
	g-ACP	98.4	10.5	3.7

$SR_{HAP\ (or\ enamel)} = (IAP/K_{sp})^{1/n}$, where K_{sp} is the corresponding thermodynamic solubility product ($pK_{SP} = -\log(K_{SP})$ equals 116.8 and 108.6 for HAP and enamel, respectively) and n is the number of ions in the IAP ($n = 18$). Indicated values represent the means of three repetitive runs

SR values > 1.00 indicate solution supersaturated with respect to HAP or enamel

4 Discussion

The results of BFS testing of ACP/UPHM composites (Fig. 1) have re-confirmed the already known fact that ACP-containing composites are too weak to be used as direct filling materials [4, 8]. For endodontic sealing applications, however, a material's mechanical strength may not be its most critical property. Though it seems improbable that conventional strength tests effectively simulate the loading and specimen geometry sealers experience in vivo, the BFS test is used here as a relative means of comparison within this class of materials.

As more and more experiments are performed with these systems, the preponderance of data begins to suggest that

dual cure formulations may be better suited for endodontic applications. The curved, oftentimes complex shape of roots can make it difficult to achieve a satisfactory depth of cure with systems using only photo-initiation—a problem which can be offset by the secondary chemical setting that takes place in dual cure systems. In addition to having a higher degree of cure than LC systems [16], the BFS of DC formulations did not differ significantly from the corresponding LC specimens. Overall BFS values of both dry and wet specimens across the four ACP/UPHM composite groups compare well with the BFS values of the experimental ACP composites formulated for application as orthodontic adhesives (4), which have demonstrated the in vitro ability to remineralize subsurface carious lesions in human teeth [7].

ACP composites are multiphase materials, so it is perhaps appropriate to speak of them as possessing a "net" hydrophilicity, or the sum of water absorbed by the resin components and the ACP filler [3, 4, 8]. Through performing concurrent relative humidity and saline immersion experiments, we can more easily differentiate the individual contributions of (and interactions between) the filler and resin phases. Relative humidity experiments separate specimen and liquid; any uptake of water is therefore driven by the intrinsic hydrophilicity of the copolymer, and mitigated by the type and amount of filler. With the exception of glass-filled composites (which contain 50% less resin than other composites), the RH data presented here exemplifies this perfectly. Significant differences in WS occur only between different resin systems, and within those systems WS decreases with decreasing particle size. The large, porous am-ACP particles are heterogeneously dispersed and do not interface well with resin. By providing paths of diffusion and absorbing water themselves, they act to increase the net hydrophilicity of composites into which they are incorporated. Grinding ACP reduces particle size, thereby increasing homogeneity and reducing filler porosity, ultimately lowering the maximum WS.

After reaching the maximum values, WS at 75% RH (Fig. 2) was maintained at practically a constant level throughout the experiment. Differently from RH experiments, the maximum WS values of immersed specimens were reached at 720 h, and reduced afterwards for (15–21) % in LC and DC ACP composite groups, 12% for LC glass composite and (5–12) % for LC and DC copolymer group (Fig. 3). The overall mass changes of the immersed composites were affected by the loss of mineral ions, which occurs as a result of ACP's spontaneous conversion to thermodynamically stable apatite in immersed composite specimens. This could, therefore, be considered as one of the processes controlling the overall mass changes observed after 720 h (1 month). An identical WS-decreasing trend after 1 month immersion was, however, observed in both copolymers and the glass control group as well. This would imply that certain resin-related processes, such as the leaching out of unreacted monomeric species and/or hydrolytic degradation products, may have played an equally important role in the overall mass changes of all immersed UPHM specimens. The polymerization shrinkage of these composite specimens, which varies between 6.9 vol.% and 7.1 vol.% [16], should be more than compensated for by the hygroscopic expansion they undergo (maximum measured volume increases were up to 14%; Fig. 4). Other groups have also demonstrated this beneficial aspect of hygroscopic expansion [21, 22], and while a recent evaluation of contemporary posterior resin-based filling materials did not [25], this is likely due to the fact that the expansion of the commercial materials tested (composed of different dimethacrylate resins with various filler types and load levels) did not exceed their volumetric shrinkage (1.3% vs. 1.6–3.7%, respectively).

The kinetics of calcium and phosphate ion release from ACP-filled composites is generally determined by the nature of the polymer matrix network structure, the copolymer's permeability to water, internal pH and the rate of ACP to apatite conversion [11]. Kinetic profiles (Fig. 5a, b) revealed high release levels within the first 8–14 days, followed by continuous but declining release for the remaining period of up to 3 months. The higher releases seen during the early time periods (1–2 weeks of immersion) are most likely due to the swelling of the polymer phase of the composites. During this period water channels within the polymer likely enlarge, facilitating rapid diffusion of water molecules [26, 27]. When the cumulative releases of calcium and phosphate from both types of ACP/UPHM composites were plotted as a function of water sorption (Fig. 7a, b), significant positive linear correlations were observed (R^2 values ranging from 0.939 to 0.971). The amounts of calcium and phosphate released in all composites were linearly proportional to the WS, with somewhat higher release rates in am-ACP composites compared to their g-ACP counterparts. The average proportionality constants of 0.14 vs. 0.09 (for calcium) and 0.30 vs. 0.19 (for phosphate), respectively, could be attributed to the existence of a higher number of water sorption-prone, subsurface voids in am-ACP composites, which generally show less homogeneous filler distribution throughout the composite [9]. Once the solution concentration data are recalculated in terms of supersaturation with respect to stoichiometric apatite and/or enamel (1 month immersion data are presented in Table 4) it can easily be demonstrated that the attained supersaturation levels were significantly above the minimum necessary for remineralization to occur (saturation ratio, SR $>$ 1.00).

Compared to our earlier formulations that utilized experimental resins based on Bis-GMA and/or EBPADMA

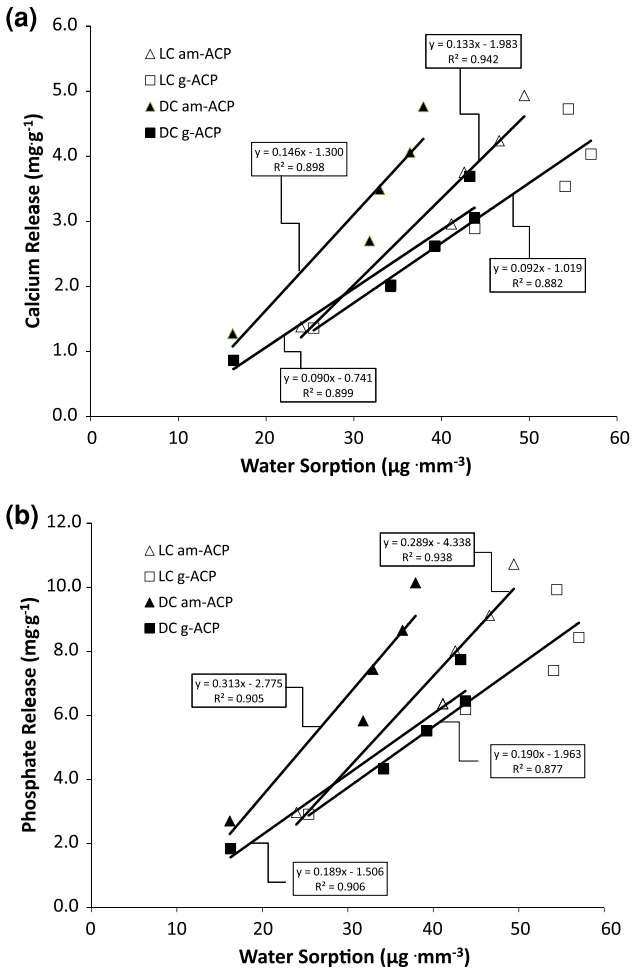

Fig. 7 Regression analysis of the cumulative calcium (**a**) and phosphate (**b**) ion release from saline-immersed specimens as a function of water sorption. Equations and the corresponding correlation coefficients are indicated for each experimental composite group

[8, 11], all ACP/UPHM composites evaluated in this study exhibited equal or higher remineralization potential, thus confirming their strong potential for preventing, or possibly even reversing root caries in endodontic applications. Physicochemical tests described in this study provide no basis for one to distinguish between the DC and LC formulations, or between the am- and g-ACP composites. However, DC g-ACP formulation should be favored due to the nature of intended application and the fact that, although not confirmed in this work, numerous earlier studies [4, 5, 8, 10, 11] have shown ground and/or milled ACP composites to be mechanically superior to as-made (coarse) ACP composites. A series of micro-leakage and quantitative leachability tests should be performed with DC g-ACP/UPHM composites before this experimental material can be recommended for testing in clinical settings.

5 Conclusion

The experimental dual-cure and light-cure urethane dimethacrylate-based ACP polymeric composites formulated for endodontic utility exhibited relatively high levels of water sorption, accompanied by a significant hygroscopic expansion. The latter may be useful in combating stresses that develop in these materials due to polymerization. Ion release profiles of the experimental materials confirmed their potential for regeneration of mineral-deficient tooth structures. Their moderate to low mechanical strength, similar to that of ACP orthodontic adhesive, did not diminish the enthusiasm for the proposed application as an endodontic sealer, for which dual-cure ground ACP composites appear to be the most adequate. Micro-leakage and quantitative leachability studies should be performed to further establish the viability of this experimental material.

Acknowledgements This investigation was supported by Research Grant DE13169-10 from the National Institute of Dental and Craniofacial Research, the National Institute of Standards and Technology and the American Dental Association Foundation. We gratefully acknowledge Esstech, Essington, PA, USA for generously providing the monomers used in this study.

References

1. Dorozhkin SV. Calcium orthophosphates in nature, biology and medicine. Materials. 2009;2:399–498.
2. Boskey AL. Amorphous calcium phosphate. The contention of bone. J Dent Res. 1997;76:1433–6.
3. Eanes ED. Amorphous calcium phosphate: termodynamic and kinetic considerations. In: Amjad Z, editor. Calcium phosphates in biological and industrial systems. Boston: Kluwer Academic Publishers; 1998. p. 21–39.
4. Antonucci JM, Skrtic D. Physicochemical properties of bioactive polymeric composites: effects of resin matrix and the type of amorphous calcium phosphate filler. In: Shalaby DW, Salz U, editors. Polymers for dental and orthopedic applications. Boca Raton: CRC Press; 2007. p. 217–42.
5. Skrtic D, Antonucci JM. Dental composites based on amorphous calcium phosphate—resin composition/physicochemical properties study. J Biomater Appl. 2007;21:375–93.
6. Skrtic D, Hailer AW, Takagi S, Antonucci JM, Eanes ED. Quantitative assessment of the efficacy of amorphous calcium phosphate/methacrylate composites in remineralizing caries-like lesions artificially produced in bovine enamel. J Dent Res. 1996; 75(9):1679–86.
7. Langhorst SE, O'Donnell JNR, Skrtic D. In vitro remineralization of enamel by polymeric amorphous calcium phosphate composite: quantitative micro-radiographic study. Dent Mater. 2009;25: 884–91.
8. Skrtic D, Antonucci JM, Eanes ED. Amorphous calcium phosphate-based bioactive polymeric composites for mineralized tissue regeneration. J Res Natl Inst Stand Technol. 2003;108(3): 167–82.
9. Skrtic D, Antonucci JM, Eanes ED, Eidelman N. Dental composites based on hybrid and surface-modified amorphous calcium phosphates—a FTIR microspectroscopic study. Biomaterials. 2004;25:1141–50.

10. Antonucci JM, Skrtic D. Matrix resin effects on selected physicohemical properties of amorphous calcium phosphate composites. J Bioact Compat Polym. 2005;20:29–49.
11. Skrtic D, Antonucci JM, Liu DW. Ethoxylated bisphenol A methacrylate-based amorphous calcium phosphate composites. Acta Biomater. 2006;2(1):85–94.
12. Tung MS, Eichmiller FC. Dental applications of amorphous calcium phosphates. J Clin Dent. 1999;10:1–6.
13. Reynolds EC, Cai F, Shen P, Walker GD. Retention in plaque and remineralization of enamel lesions by various forms of calcium in a mouthrinse or sugar-free chewing gum. J Dent Res. 2003;82(3): 206–11.
14. Mazzaoui SA, Burrow MF, Tyas MJ, Dashper SG, Eakins D, Reynolds EC. Incorporation of casein phosphopeptide-amorphous calcium phosphate into a glass-ionomer cement. J Dent Res. 2003;82(11):914–8.
15. Antonucci JM, Skrtic D, Eanes ED. Polymeric amorphous calcium phosphate compositions. U.S. Letters Patent 1996;5,508, 342:April 16.
16. O'Donnell JNR, Skrtic D. Degree of vinyl conversion, polymerization shrinkage and stress development in experimental endodontic composite. J Biomim Biomater Tissue Eng. (in press).
17. Söderholm KJ, Zigan M, Ragan M, Fischlschweiger W, Bergman M. Hydrolytic degradation of dental composites. J Dent Res. 1984;63:1248–54.
18. Berglund A, Hulterström AK, Gruffman E, van Dijken JWV. Dimensional change of calcium aluminate cement for posterior restorations in aqueous and dry media. Dent Mater. 2006;22: 470–6.
19. Feilzer AJ, de Gee AJ, Davidson CL. Relaxation of polymerization contraction shear stress by hygroscopic expansion. J Dent Res. 1990;69:36–9.
20. Attin T, Buchalla W, Kiebassa AM, Hellwig E. Curing shrinkage and volumetric changes of resin-modified glass ionomer restorative materials. Dent Mater. 1995;11:359–62.
21. Huang C, Tay FR, Cheung GSP, Kei LH, Wei SHY, Pashley DH. Hygroscopic expansion of a compomer and a composite on artificial gap reduction. J Dent. 2002;30:11–9.
22. Momoi Y, McCabe JF. Hygroscopic expansion of resin based composites during 6 months of water storage. Br Dent J. 1994; 176:91–6.
23. Antilla EJ, Krintila OH, Laurila TK, Lassila LVJ, Vallittu PK, Hernberg RGR. Evaluation of polymerization shrinkage and hygroscopic expansion of fiber-reinforced biocomposites using optical fiber Bragg grating sensors. Dent Mater. 2008;24:1720–7.
24. ASTM F394-78 (re-approved 1991). Standard test method for biaxial strength (modulus of rupture) of ceramic substrates.
25. Rüttermann S, Krüger S, Raab WHM, Janda R. Polymerization shrinkage and hygroscopic expansion of contemporary posterior resin-based filling materials—a comparative study. J Dent. 2007; 35:806–13.
26. Wadgaonkar B, Ito S, Svizero N, Elrod D, Foulger S, Rodgers R, et al. Evaluation of the effect of water-uptake on the compendance of dental resins. Biomaterials. 2006;27:3287–94.
27. Hirashi N, Yiu CKY, King NM, Tay FR, Pashley DH. Chlorhexidine release and water sorption characteristics of chlorhexidine-incorporated hydrophobic/hydrophilic resins. Dent Mater. 2008;24:1391–9.